J. Fluid Mech. (1983), vol. 132, 445–455
Printed in Great Britain

Low-Reynolds-number flow past a cylindrical body

By KO TAMADA,
Department of Mechanical Engineering, Osaka Industrial University, Daito, Japan

HIROYUKI MIURA
Department of Mathematical Sciences, University of Osaka Prefecture, Sakai, Japan

AND TOSIO MIYAGI
Department of Aeronautical Engineering, University of Osaka Prefecture, Sakai, Japan

(Received 25 November 1982)

Two-dimensional flow past a cylindrical body of arbitrary profile at small Reynolds numbers is studied theoretically. The asymptotic flow field at large distances from an immersed body is shown to depend only upon the force acting on the cylinder. This universal field is determined by solving the Navier–Stokes equation numerically. The result enables us to evaluate the force acting on the body as a function of the flow Reynolds number. A detailed calculation is made of the drag coefficients of a circular cylinder and a flat plate. Results compare favourably with existing experimental and numerical data.

1. Introduction

Viscous forces are dominant over inertial forces near a body placed in an otherwise uniform flow when the Reynolds number of the flow is small. Total neglect of the inertial forces, however, causes some contradiction, since inertial forces become comparable with viscous forces at large distances from the immersed body. In the two-dimensional case, the Stokes approximation neglecting inertial effects leads to logarithmic divergence of the flow velocity at infinity. Oseen (1910) proposed a method to remove this difficulty by retaining the inertial terms in a linearized form, and Lamb (1911) obtained a reasonable result for a circular cylinder by solving Oseen's equation approximately.

Important contributions were made by Kaplun (1957) and Proudman & Pearson (1957) by applying the singular-perturbation method to the full Navier–Stokes equation. They distinguished the Stokes region around the body, where viscous forces are dominant, from the Oseen region, where inertial forces are comparable with viscous forces. Approximate solutions in respective regions were so determined that they match with each other in an intermediate region. The result was expressed in a power series essentially in $|\ln R|^{-1}$, where R is the Reynolds number. Kaplun advanced his calculation up to $|\ln R|^{-2}$. In addition, Lamb's drag formula was found to be correct to $|\ln R|^{-1}$.

We may consider the situation in which $|\ln R|^{-1}$ is not small while R is still small. In this case, all the successive terms in Kaplun's expansion are of the same order, and his assumption that the deviation from the uniform flow is small in the Oseen region does not hold. Thus the flow outside the Stokes region should obey the full Navier–Stokes equation instead of the Oseen equation. In the present paper, we

15-2

analyse such a case in order to get better results in a wider range of the Reynolds number than in Kaplun's analysis.

2. Analytical considerations

The motion of a viscous fluid obeys the equation of continuity and the Navier–Stokes equation. These equations for the steady two-dimensional flow past a cylindrical body may be written in terms of dimensionless variables as

$$\frac{\partial u}{\partial x}+\frac{\partial v}{\partial y}=0, \tag{1}$$

$$R\left(u\frac{\partial}{\partial x}+v\frac{\partial}{\partial y}\right)\hat{\omega}=\left(\frac{\partial^2}{\partial x^2}+\frac{\partial^2}{\partial y^2}\right)\hat{\omega},\quad \hat{\omega}=\frac{\partial v}{\partial x}-\frac{\partial u}{\partial y}. \tag{2}$$

Here (x,y) are Cartesian coordinates and (u,v) the velocity components, each normalized by a characteristic length L of the body and the undisturbed velocity U respectively. Also, $\hat{\omega}$ is the dimensionless vorticity and R the Reynolds number based on L and U. The uniform flow is in the x-direction.

In the neighbourhood of the body where $r\equiv(x^2+y^2)^{\frac{1}{2}}=O(1)$, the inertial terms can be neglected for small R, and (2) reduces to the Stokes equation

$$\left(\frac{\partial^2}{\partial x^2}+\frac{\partial^2}{\partial y^2}\right)\hat{\omega}=0. \tag{3}$$

Since the body shrinks to a point in a large-scale view, the solution of (3) satisfying the no-slip condition on the body surface takes a universal form known as a Stokeslet at large r. Thus the complex velocity takes the form (Tamada 1957)

$$u-\mathrm{i}v\sim 2\bar{A}\ln r-A\,\mathrm{e}^{-2\mathrm{i}\theta}+\tau\quad (r\gg 1), \tag{4}$$

where $\theta\equiv\tan^{-1}(y/x)$ and A and τ are certain constants, $\bar{A}$ being the complex conjugate of A. The constant A is connected with the force per unit length acting on the cylinder as follows:

$$F_x+\mathrm{i}F_y=8\pi\mu UA, \tag{5}$$

where (F_x,F_y) are the (x,y)-components of the force, and μ is the viscosity coefficient. Another constant τ depends on A and $\bar{A}$ linearly as

$$\tau=\mathcal{A}A+\mathcal{B}\bar{A}, \tag{6a}$$

where $\mathcal{A}$ and $\mathcal{B}$ are related to the geometric properties of the cylinder. In the case of an elliptic cylinder, for example, we have (see the appendix; Hasimoto 1953; Imai 1954; Tamada 1957)

$$\mathcal{A}=\frac{1-\delta}{1+\delta}\mathrm{e}^{2\mathrm{i}\alpha},\quad \mathcal{B}=-2\ln\{\tfrac{1}{4}(1+\delta)\}, \tag{6b}$$

where the major axis is taken as the characteristic length of the cylinder, δ is the ratio of minor to major axis and α is the angle between the major and x-axes.

Viscous forces become so small in the far field of $r=O(R^{-1})$ as to be comparable with inertial forces. To describe the fluid motion in this outer region, we use shrunk coordinates defined as

$$\tilde{x}=Rx,\quad \tilde{y}=Ry. \tag{7}$$

Then (1) and (2) are transformed into forms free from R:

$$\frac{\partial u}{\partial \tilde{x}}+\frac{\partial v}{\partial \tilde{y}}=0, \tag{8}$$

$$\left(u\frac{\partial}{\partial \tilde{x}}+v\frac{\partial}{\partial \tilde{y}}\right)\tilde{\omega}=\left(\frac{\partial^2}{\partial \tilde{x}^2}+\frac{\partial^2}{\partial \tilde{y}^2}\right)\tilde{\omega}, \quad \tilde{\omega}=\frac{\partial v}{\partial \tilde{x}}-\frac{\partial u}{\partial \tilde{y}}. \tag{9}$$

The flow in the outer region where $\tilde{r} \equiv (\tilde{x}^2+\tilde{y}^2)^{\frac{1}{2}} = O(1)$ is thus governed by the full Navier–Stokes equation. The solution for the outer region should match with the previous solution for the Stokes region in an overlap domain of validity where $R \ll \tilde{r} \ll 1$. Another condition is that the flow approaches the uniform flow at infinity. Thus the outer solution can be obtained by solving (8) and (9) subject to the following boundary conditions:

$$u-\mathrm{i}v \sim 2\bar{A}\ln\tilde{r}-A\,\mathrm{e}^{-2\mathrm{i}\theta}+\text{constant} \quad \text{as} \quad \tilde{r}\to 0, \tag{10}$$

$$u-\mathrm{i}v \to 1 \quad \text{as} \quad \tilde{r}\to\infty, \tag{11}$$

where A is the force coefficient (cf. (4), (5)). These conditions mean that the outer solution represents the flow induced by a Stokeslet singularity placed at a point in a uniform flow. It depends only upon the intensity of the singularity or A and $\bar{A}$. Once this solution is found, we may have its expansion form for $\tilde{r} \ll 1$ such as

$$u-\mathrm{i}v = 2\bar{A}\ln\tilde{r}-A\,\mathrm{e}^{-2\mathrm{i}\theta}+K+O[\tilde{r}(\ln\tilde{r})^2]. \tag{12}$$

Here the constant K, a complex quantity in general, is a universal function of $A, \bar{A}$ and will take a major role in the present study. Now, if we rewrite (4) in terms of (7), the resulting expression should agree with (12) by the matching principle. Thus we have the relation

$$R = \exp\frac{\tau-K}{2\bar{A}}. \tag{13}$$

Inserting τ and K (both known functions of A and $\bar{A}$) into (13) and solving for A as a function of R, we can obtain the force acting on the cylinder from (5).

In the case when $|\ln R|^{-1}$ is small, the outer solution can be constructed analytically by successive approximation of the Oseen type as mentioned earlier. Its first approximation is seen to be a fundamental solution of the Oseen equation (Oseenlet) responsible for the force (5), i.e.

$$u-\mathrm{i}v = 1-2\exp\left(\tfrac{1}{2}\tilde{x}\right)\{\bar{A}K_0(\tfrac{1}{2}\tilde{r})+AK_1(\tfrac{1}{2}\tilde{r})\,\mathrm{e}^{-\mathrm{i}\theta}\}+4A\tilde{r}^{-1}\,\mathrm{e}^{-\mathrm{i}\theta}, \tag{14}$$

where K_0 and K_1 are modified Bessel functions. If we expand this for $\tilde{r} \ll 1$ and compare the result with (12), we get the first approximation to $K(A, \bar{A})$ as

$$K = 1-A-2(\ln 4-\gamma)\bar{A}, \tag{15}$$

where $\gamma = 0.57721\ldots$ is Euler's constant. In the case when the cylinder under consideration experiences no lift force, A is real and (15) becomes

$$K = 1-2(\ln 4-\gamma+\tfrac{1}{2})A. \tag{16}$$

The solution (14) is correct to $O(A)$. It can be shown that (16) leads to Lamb's (1911) drag formula for a circular cylinder. We may proceed to higher approximations by assuming the solution in a power series in A and $\bar{A}$. Kaplun's (1957) analysis corresponds to the approximation correct to $O(A^2)$. Further progress along this line is, however, very difficult, if not impossible. We then appeal in the present study to numerical procedures in solving (8) and (9) under the conditions (10) and (11). This approach may enable us to obtain the universal outer solution and hence the function $K(\Lambda, \bar{\Lambda})$, which are exact within the accuracy of the numerical method used.

3. Numerical calculation

We restrict our numerical analysis to a simple case when the cross-section of the cylinder is symmetric with respect to the x-axis. All of Λ, τ and K are real in this case.

The stream function ψ for the deviation from the uniform flow is introduced as

$$u = 1 - 2\Lambda \frac{\partial \psi}{\partial \tilde{y}}, \quad v = 2\Lambda \frac{\partial \psi}{\partial \tilde{x}}. \tag{17}$$

It is suitable to use modified polar coordinates (ξ, θ) for numerical calculation of the flow field for small $\tilde{r}$, where

$$\xi = \ln \tilde{r}. \tag{18}$$

The Navier–Stokes equation (9) is written in terms of these variables as

$$\frac{\partial^2 \omega}{\partial \xi^2} + \frac{\partial^2 \omega}{\partial \theta^2} = \left(e^{\xi} \cos\theta - 2\Lambda \frac{\partial \psi}{\partial \theta}\right) \frac{\partial \omega}{\partial \xi} - \left(e^{\xi} \sin\theta - 2\Lambda \frac{\partial \psi}{\partial \xi}\right) \frac{\partial \omega}{\partial \theta}, \tag{19a}$$

$$\frac{\partial^2 \psi}{\partial \xi^2} + \frac{\partial^2 \psi}{\partial \theta^2} = -e^{2\xi} \omega. \tag{19b}$$

The inner boundary condition (10) or (12) takes the form

$$\omega \sim 2 e^{-\xi} \sin\theta, \quad \psi \sim (-\xi + \kappa) e^{\xi} \sin\theta \quad \text{as} \quad \xi \to -\infty, \tag{20}$$

where

$$\kappa = \frac{1-K}{2\Lambda} + \tfrac{1}{2}. \tag{21}$$

The condition for the flow symmetry is given by

$$\omega = \psi = 0 \quad (\theta = 0, \pi). \tag{22}$$

We apply the successive over-relaxation method (cf. Roache 1976) to solve (19). The numerical procedure is expressed by the finite-difference formulae to second-order accuracy as

$$\omega_{ij}^{(n+1)} = \omega_{ij}^{(n)} + \beta[\omega_{i+1,j} + \omega_{i-1,j} + \omega_{i,j+1} + \omega_{i,j-1} - 4\omega_{ij} - C_{\xi}(\omega_{i+1,j} - \omega_{i-1,j}) + C_{\theta}(\omega_{i,j+1} - \omega_{i,j-1})], \tag{23a}$$

$$\psi_{ij}^{(n+1)} = \psi_{ij}^{(n)} + \beta'[\psi_{i+1,j} + \psi_{i-1,j} + \psi_{i,j+1} + \psi_{i,j-1} - 4\psi_{ij} + e^{2\xi} h^2 \omega_{ij}], \tag{23b}$$

where

$$C_{\xi} = \tfrac{1}{2} e^{\xi} h \cos\theta - \tfrac{1}{2}\Lambda(\psi_{i,j+1} - \psi_{i,j-1}), \tag{24a}$$

$$C_{\theta} = \tfrac{1}{2} e^{\xi} h \sin\theta - \tfrac{1}{2}\Lambda(\psi_{i+1,j} - \psi_{i-1,j}), \tag{24b}$$

the superscript n refers to the values at the nth iteration, (i,j) refer to the grid point on the (ξ, θ)-plane and h is the grid scale. To ensure numerical convergence, we have chosen the over-relaxation factors β and β' as

$$\beta = 0.9\{2 + 2^{\frac{1}{2}}(|C_{\xi}| + |C_{\theta}|)\}^{-1}, \quad \beta' = 0.45. \tag{25}$$

The condition (20) for ψ as $\xi \to -\infty$ may be changed into a form free from the unknown κ:

$$\frac{\partial}{\partial \xi}\left(\frac{\psi}{\mathrm{e}^{\xi}\sin\theta}\right) \sim -1 \quad \text{as} \quad \xi \to -\infty. \tag{26}$$

Using this formula, we can calculate ψ at a computational boundary $\xi = \xi_0$ (say) as follows:

$$\psi(\xi_0, \theta) = \mathrm{e}^{-2h}\,\psi(\xi_0 + 2h, \theta) + 2h\,\mathrm{e}^{\xi_0}\sin\theta. \tag{27}$$

Once we get the converged solution for a given Λ after iterations, κ can be found through the formula

$$\kappa = \frac{2}{\pi}\mathrm{e}^{-\xi_0}\int_0^{\pi}\psi(\xi_0, \theta)\sin\theta\,\mathrm{d}\theta + \xi_0. \tag{28}$$

This method of determining κ is more effective than the method of trial and error using (20) as it is.

The use of polar coordinates is inadequate for numerical treatment of the flow at large $\tilde{r}$ because the vortical wake is confined to a narrow strip along $\theta = 0$. Finer grid scales for θ are required at larger $\tilde{r}$ to describe the flow change correctly, which may produce much complication in the numerical calculation. Appropriate coordinates for the vortical region at large $\tilde{r}$ may be the parabolic coordinates (ζ, η), where

$$\zeta = (\tilde{r} + \tilde{x})^{\frac{1}{2}}, \quad \eta = (\tilde{r} - \tilde{x})^{\frac{1}{2}}. \tag{29}$$

The Navier–Stokes equation (9) is transformed with (17) and (29) into

$$\frac{\partial^2 \omega}{\partial \zeta^2} + \frac{\partial^2 \omega}{\partial \eta^2} = \left(\zeta - 2\Lambda\frac{\partial \psi}{\partial \eta}\right)\frac{\partial \omega}{\partial \zeta} - \left(\eta - 2\Lambda\frac{\partial \psi}{\partial \zeta}\right)\frac{\partial \omega}{\partial \eta}, \tag{30a}$$

$$\frac{\partial^2 \psi}{\partial \zeta^2} + \frac{\partial^2 \psi}{\partial \eta^2} = -(\zeta^2 + \eta^2)\,\omega. \tag{30b}$$

Instead of the boundary condition (11) at infinity, we actually use the asymptotic formulae obtained by Imai (1951):

$$\omega \sim 2^{\frac{3}{2}}\pi^{\frac{1}{2}}\zeta^{-2}\eta\exp\left(-\tfrac{1}{2}\eta^2\right) - 2^{\frac{5}{2}}\pi\Lambda\zeta^{-3}\left[\pi^{\frac{1}{2}}(1-\eta^2)\exp\left(-\tfrac{1}{2}\eta^2\right)\operatorname{erf}\left(2^{-\frac{1}{2}}\eta\right) - 2^{\frac{1}{2}}\eta\exp\left(-\eta^2\right)\right], \tag{31a}$$

$$\psi \sim 2\pi\operatorname{erf}\left(2^{-\frac{1}{2}}\eta\right) - 4\tan^{-1}\left(\zeta^{-1}\eta\right) + 2^{\frac{5}{2}}\pi^{\frac{3}{2}}\Lambda\zeta^{-1}\left[2^{\frac{1}{2}}\{\operatorname{erf}(\eta) - 1\} - \exp\left(-\tfrac{1}{2}\eta^2\right)\operatorname{erf}\left(2^{-\frac{1}{2}}\eta\right)\right] + 8\pi^{\frac{3}{2}}\Lambda\zeta(\zeta^2+\eta^2)^{-1}. \tag{31b}$$

Use of (31) permits us to put the computational boundary $\zeta = \zeta_\infty$ or $\eta = \eta_\infty$ corresponding to infinity at distances nearer the origin (Takami & Keller 1969). Also, (31) implies that the vorticity becomes small exponentially as η increases. For computational efficiency, we put $\omega = 0$ in the region where η is greater than some value η_* and solve only the Laplace equation for ψ there.

With reference to the asymptotic formulae (31), we have performed practical calculations with the independent variables defined as

$$\tilde{\zeta} = \ln(1+\zeta), \tag{32a}$$

$$\tilde{\eta} = \eta + \tfrac{1}{2}\eta^2 \quad (\eta < \eta_*), \tag{32b}$$

$$\eta' = \tfrac{1}{2}\ln\tilde{\eta} \quad (\eta \geqslant \eta_*), \tag{32c}$$

in order to retain the accuracy to second order. We compute ω and ψ according to the formula (23) for $\xi_0 < \xi \leqslant \xi_*$ (say) and to similar formulae for the equations resulting with the coordinates (32) in the domain where $\zeta^2+\eta^2 > 2\exp(\xi_*)$, $0 < \zeta < \zeta_\infty$ and $0 < \eta < \eta_\infty$. A computational problem is how to calculate ω and ψ at $\xi = \xi_*$, where (23) contains the unspecified terms, i.e. $\omega(\xi_*+h, \theta)$ and $\psi(\xi_*+h,\theta)$. We have to give them correctly to $O(h^3)$ so that (23) may represent (19) to second-order accuracy. Let (i,j) denote the grid point on the $(\tilde{\zeta},\tilde{\eta})$-plane which stands close to the point corresponding to (ξ_*+h,θ) and $(\Delta\tilde{\zeta},\Delta\tilde{\eta})$ be the increments between the two points. Taylor expansion at the point (i,j) yields

$$q(\xi_*+h,\theta) = q_{ij}+\sum_{n=1}^{3}\frac{1}{n!}\left(-\Delta\tilde{\zeta}\frac{\partial}{\partial\tilde{\zeta}}-\Delta\tilde{\eta}\frac{\partial}{\partial\tilde{\eta}}\right)^n q\bigg|_{ij}+O(h^4), \tag{33}$$

where q stands for ω or ψ. The derivatives on the right-hand side can be calculated as

$$q_{\tilde{\zeta}\tilde{\zeta}\tilde{\zeta}} = \tilde{h}^{-3}(q_{i+3,j}-3q_{i+2,j}+3q_{i+1,j}-q_{ij}), \tag{34a}$$

$$q_{\tilde{\zeta}\tilde{\zeta}} = \tilde{h}^{-2}(-q_{i+3,j}+4q_{i+2,j}-5q_{i+1,j}+2q_{ij}), \tag{34b}$$

$$q_{\tilde{\zeta}} = (6\tilde{h})^{-1}(2q_{i+3,j}-9q_{i+2,j}+18q_{i+1,j}-11q_{ij}), \tag{34c}$$

$$q_{\tilde{\zeta}\tilde{\zeta}\tilde{\eta}} = (\tilde{h}^2\tilde{k})^{-1}(q_{i+2,j+1}-q_{i+2,j}-2q_{i+1,j+1}+2q_{i+1,j}+q_{i,j+1}-q_{ij}), \tag{34d}$$

$$q_{\tilde{\zeta}\tilde{\eta}} = (2\tilde{h}\tilde{k})^{-1}(-q_{i+2,j+1}+q_{i+2,j}-q_{i+1,j+2}+6q_{i+1,j+1}-5q_{i+1,j}+q_{i,j+2} -5q_{i,j+1}+4q_{ij})$$

$$\text{etc.,} \tag{34e}$$

where $(\tilde{h},\tilde{k})$ are the grid scales for $(\tilde{\zeta},\tilde{\eta})$ respectively. Computing ω and ψ at the grid points just outside $\zeta^2+\eta^2 = 2\exp(\xi_*)$ on the $(\tilde{\zeta},\tilde{\eta})$-plane, we can give the unspecified terms in a similar way using the values specified at the grid points on the (ξ,θ)-plane.

We have chosen $\xi_0 = -2\pi$, $\xi_* = \frac{1}{4}\pi$, $\eta_* \approx 4.0$, $\eta_\infty \approx 30$ and $\zeta_\infty \approx 30$ in the present calculation and iterated to compute ω and ψ from $\xi = \xi_0$ to $\xi = \xi_*$, from $\zeta = 0$ to $\zeta = \zeta_\infty$ and in the opposite direction. Convergence was assumed when $|\kappa^{(n)}-\kappa^{(n-1)}|$ became less than 3×10^{-5}. The grid scales are taken as

$$h = \frac{\pi}{m}, \quad \tilde{h} = \frac{1}{m}\ln\{1+2^{\frac{1}{2}}\exp(\tfrac{1}{2}\xi_*)\},$$

$$\tilde{k} = \frac{1}{m}\{2^{\frac{1}{2}}\exp(\tfrac{1}{2}\xi_*)+\exp(\xi_*)\}, \quad k' = -\tfrac{1}{2}\ln\{1-6\tilde{k}(\eta_*+\tfrac{1}{2}\eta_*^2)^{-1}\},$$

where m is an integer and k' is the grid scale for η'. The result for $m = 12$, 16 over $0 \leqslant \Lambda \leqslant 0.5$ are shown in table 1. The exact value for $\Lambda = 0$ can be found from Lamb's result (16) with (21) as

$$\kappa(0) = \ln 4-\gamma+1 \approx 1.809. \tag{35}$$

Our numerical results may contain errors $O(h^2)$. It appears that the deviation of our results for $\Lambda = 0$ from the exact value is almost proportional to h^2. This was confirmed by another result of $\kappa(0) = 1.930$ for $m = 20$. Therefore we get the final results by extrapolation as

$$\kappa = \tfrac{1}{7}[16\kappa(m = 16)-9\kappa(m = 12)]. \tag{36}$$

Variation of κ with Λ is shown in figure 1 together with the results of Lamb and of Kaplun. It can be seen that Kaplun's result deviates from the present result for $\Lambda > 0.15$.

Λ	$\kappa(m = 12)$	$\kappa(m = 16)$	κ(extrapolated)
0	2.117	1.989	1.824
0.05	2.217	2.084	1.913
0.1	2.324	2.187	2.011
0.15	2.436	2.294	2.111
0.2	2.553	2.406	2.217
0.25	2.671	2.519	2.324
0.3	2.781	2.625	2.424
0.35	2.871	2.713	2.510
0.4	2.924	2.767	2.565
0.45	2.929	2.777	2.582
0.5	2.887	2.742	2.556

TABLE 1. Numerical results for $\kappa(\Lambda)$

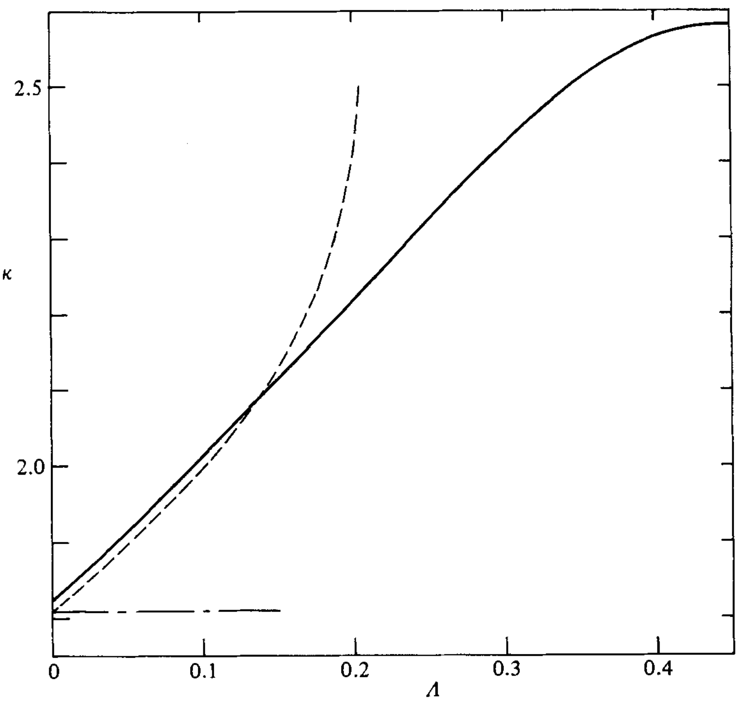

FIGURE 1. Variation of κ with Λ: ——, present result; - - -, Lamb (1911); — - —, Kaplun (1957).

4. Comparison of theoretical and experimental results for drag coefficients

The drag coefficient C_D is expressed from (5) in terms of Λ and the Reynolds number as

$$C_D \equiv \frac{F_x}{\frac{1}{2}\rho U^2 L} = \frac{16\pi\Lambda}{R}, \tag{37}$$

where ρ is the fluid density. Using the universal function $\kappa(\Lambda)$, we can represent the Reynolds number as a function of Λ through (13) and (21), if the cross-section of the cylinder is specified. As a result, we can find the relation between C_D and R with Λ as a parameter.

In the case of a circular cylinder, we have $\tau = (2\ln 2)\Lambda$ on putting $\delta = 1$ in (6).

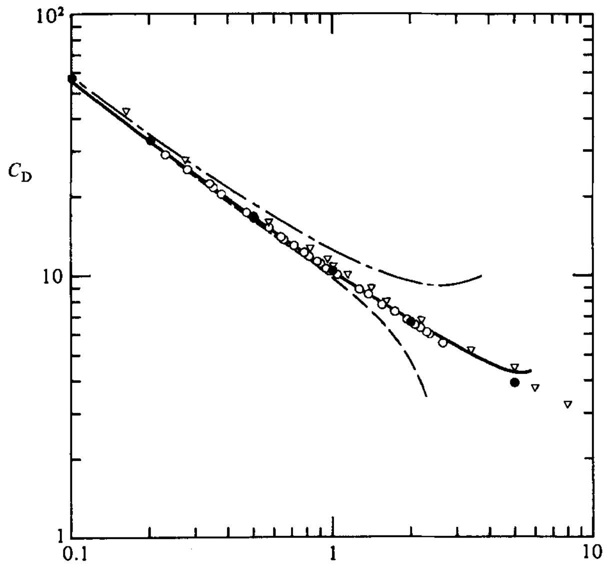

FIGURE 2. Variation of drag coefficient with Reynolds number for a circular cylinder: ——, present result; - - -, Lamb (1911); – – –, Kaplun (1957); ▽, Jayaweera & Mason (1965); ○, Huner & Hussey (1977); ●, Schlamp *et al.* (1975).

The variation of C_D with R for a circular cylinder is shown in figure 2. The analytical results of Lamb (1911) and Kaplun (1957), numerical results of Schlamp, Pruppacher & Hamielec (1975) and experimental results of Jayaweera & Mason (1965) and Huner & Hussey (1977) are also shown for comparison. The present result agrees quite well with the experimental results for $R < 5$. On the other hand, the results of Lamb and of Kaplun are valid over more restricted range of R than the present one.

The case of a flat plate is considered next, for which $\delta = 0$ in (6). We have $\tau = (2 \ln 4 \pm 1) A$ for a flat plate placed tangential or normal to the uniform stream, respectively. Figure 3 shows the variations of C_D with R in these cases. The present result for a tangential flat plate agrees well with the numerical results of Dennis & Dunwoody (1966) and the experimental results of Schaaf & Sherman (1954) for $R < 10$. Close agreement between the present result and the experimental results of Coudeville, Trepaud & Brun (1965) is also seen in the case of a normal flat plate. These experiments for a flat plate were performed using a gas of low density, and we have picked up only the data that contained negligible effects of rarefaction. As is seen from the figure, the present analysis leads to more accurate results than approximate Oseen solutions for a flat plate obtained by Harrison (1923) and Bairstow, Cave & Lang (1923).

It may be noted that our method can be applied to the case of any other profile. The only quantity that depends on the geometric properties of the body is τ. We can express it as a function of A and $\bar{A}$ exactly or approximately as the case may be using complex-variable analysis to solve the Stokes equation under no-slip condition at the body surface (see the appendix; Tamada 1957; Miura 1971).

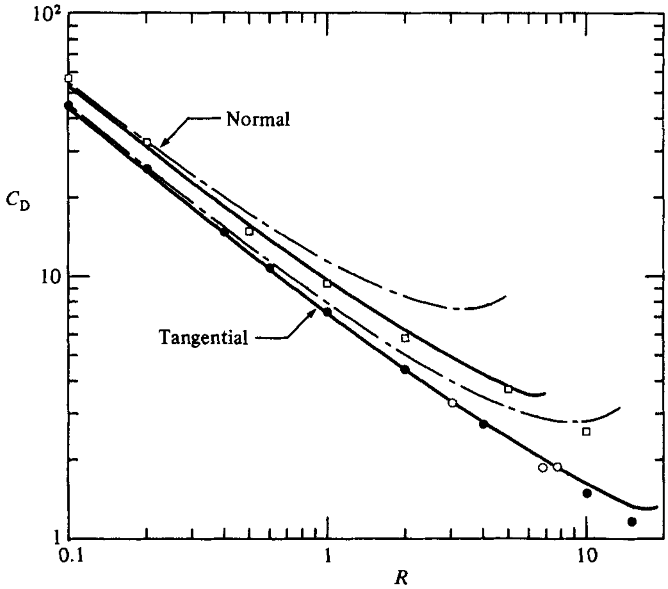

FIGURE 3. Variation of drag coefficient with Reynolds number for a flat plate: ——, present results; ---, Harrison (1923) and Bairstow *et al.* (1923); ○, Schaaf & Sherman (1954); ●, Dennis & Dunwoody (1966); □, Coudeville *et al.* (1965).

5. Conclusion

A universal asymptotic field has been analysed in two-dimensional flow past a cylindrical body at small Reynolds numbers. The universality arises from the fact that an immersed body is equivalent to a Stokeslet at large distances. The outer flow field is governed by the full Navier–Stokes equation provided that the Reynolds number is not very small. With the aid of numerical technique, we could fix the asymptotic flow field which matches with the Stokeslet flow at the origin as well as the uniform flow at infinity. The result was used to determine the relation of the force experienced by the cylinder to the Reynolds number for a cylinder of arbitrary cross-section.

The present result may correspond to Kaplun's solution when all the terms were taken in his expansion formula in $|\ln R|^{-1}$. As a result, close agreement with existing data of experiment for drag coefficient was observed in the cases of a circular cylinder and a flat plate. The range of validity extends to larger Reynolds numbers than Kaplun's analysis. This is brought about by taking the full Navier–Stokes equation in the outer flow field.

Appendix. Stokes flow past an elliptic cylinder

We consider an elliptic profile in the $z = x+iy$ plane with its centre at $z = 0$. The major axis whose length is normalized to 1 makes an angle α with the x-axis. Use is made of a Joukowski mapping

$$z = \tfrac{1}{4}(1+\delta)\,e^{-i\alpha}(\zeta+\sigma\zeta^{-1}), \quad \sigma = \frac{1-\delta}{1+\delta}, \tag{A 1}$$

which transforms the profile on to a unit circle in the ζ-plane. Here δ is the thickness ratio of the ellipse.

The complex velocity satisfying the Stokes equation may be expressed as

$$u-\mathrm{i}v = \bar{z}\frac{\mathrm{d}f}{\mathrm{d}z} - \bar{f}(\bar{z}) + g(z)$$

$$= \bar{z}(\bar{\zeta})\frac{\mathrm{d}f}{\mathrm{d}\zeta}\left(\frac{\mathrm{d}z}{\mathrm{d}\zeta}\right)^{-1} - \bar{f}(\bar{\zeta}) + g(\zeta), \tag{A 2}$$

where $f(z)$ and $g(z)$ are arbitrary analytic functions of z, and $\bar{f}(\bar{z})$ etc. are conjugate complex of $f(z)$ etc. Appropriate forms of f and g for the present problem are (Tamada 1957)

$$f(\zeta) = -A\ln\zeta + F(\zeta), \tag{A 3a}$$

$$g(\zeta) = \bar{A}\ln\zeta + \tau_* + G(\zeta), \tag{A 3b}$$

where $F(\zeta)$ and $G(\zeta)$ are regular in $|\zeta| \geqslant 1$ and both vanish as $\zeta \to \infty$, A is the force coefficient defined by (5) in the main text, and τ_* is a constant to be determined below. The boundary condition is $u - \mathrm{i}v = 0$ on $|\zeta| = 1$ ($\bar{\zeta} = \zeta^{-1}$), or

$$\bar{z}(\zeta^{-1})\frac{\mathrm{d}f}{\mathrm{d}\zeta}\left(\frac{\mathrm{d}z}{\mathrm{d}\zeta}\right)^{-1} - \bar{f}(\zeta^{-1}) + g(\zeta) = 0. \tag{A 4}$$

Substituting (A 3), we have

$$\bar{z}(\zeta^{-1})\left(-A\zeta^{-1} + \frac{\mathrm{d}F}{\mathrm{d}\zeta}\right)\left(\frac{\mathrm{d}z}{\mathrm{d}\zeta}\right)^{-1} - \bar{F}(\zeta^{-1}) + \tau_* + G(\zeta) = 0. \tag{A 5}$$

Every term on the left-hand side is regular in $|\zeta| \geqslant 1$ except for $\bar{F}(\zeta^{-1})$. Therefore $\bar{F}(\zeta^{-1})$ itself must be regular in $|\zeta| \geqslant 1$ and it is also regular in $|\zeta| \leqslant 1$ by (A 3), so that it must be a constant which is seen to be zero since $F(\infty) = 0$. Thus

$$\bar{F}(\zeta^{-1}) = 0 \quad \text{or} \quad F(\zeta) = 0. \tag{A 6}$$

Insertion of this into (A 5) yields

$$G(\zeta) = A\zeta^{-1}\bar{z}(\zeta^{-1})\left(\frac{\mathrm{d}z}{\mathrm{d}\zeta}\right)^{-1} - \tau_*. \tag{A 7}$$

From (A 3), (A 6), (A 7) and (A 1), we have

$$f(\zeta) = -A\ln\zeta, \tag{A 8a}$$

$$g(\zeta) = \bar{A}\ln\zeta + A\,\mathrm{e}^{2\mathrm{i}\alpha}\frac{\sigma\zeta^2+1}{\zeta^2-\sigma}, \quad \tau_* = \sigma A\,\mathrm{e}^{2\mathrm{i}\alpha}. \tag{A 8b}$$

If we substitute these results into (A 2), we obtain the complex velocity field around the elliptic cylinder as follows:

$$u-\mathrm{i}v = A\,\mathrm{e}^{2\mathrm{i}\alpha}\frac{(\zeta\bar{\zeta}-1)(\sigma\zeta-\bar{\zeta})}{\bar{\zeta}(\zeta^2-\sigma)} + \bar{A}\ln(\zeta\bar{\zeta}). \tag{A 9}$$

When $|\zeta| \gg 1$, $\zeta \sim 4\,\mathrm{e}^{\mathrm{i}\alpha}(1+\delta)^{-1}z$ from (A 1), and hence

$$u-\mathrm{i}v \sim 2\bar{A}\ln r - A\,\mathrm{e}^{-2\mathrm{i}\theta} + \sigma A\,\mathrm{e}^{2\mathrm{i}\alpha} - 2\bar{A}\ln\{\tfrac{1}{4}(1+\delta)\}. \tag{A 10}$$

Comparing this with (4) in the main text, we reach the result (6).

REFERENCES

Bairstow, L., Cave, B. M. & Lang, E. D. 1923 *Phil. Trans. R. Soc. Lond.* **A223,** 383.

Coudeville, H., Trepaud, P. & Brun, E. A. 1965 In *Rarefied Gas Dynamics*, vol. 1 (ed. J. H. de Leeuw), p. 444.

Dennis, S. C. R. & Dunwoody, J. 1966 *J. Fluid Mech.* **24**, 577.

Harrison, W. J. 1923 *Trans. Camb. Phil. Soc.* **23**, 71.

Hasimoto, H. 1953 *J. Phys. Soc. Japan* **8**, 653.

Huner, B. & Hussey, R. G. 1977 *Phys. Fluids* **20**, 1211.

Imai, I. 1951 *Proc. R. Soc. Lond.* **A208**, 487.

Imai, I. 1954 *Proc. R. Soc. Lond.* **A224**, 141.

Jayaweera, K. O. L. F. & Mason, B. J. 1965 *J. Fluid Mech.* **22**, 709.

Kaplun, S. 1957 *J. Maths Mech.* **6**, 595.

Lamb, H. 1911 *Phil. Mag.* **21**, 112.

Miura, H. 1971 *Bull. Univ. Osaka Prefecture* **A20**, 215.

Oseen, C. W. 1910 *Ark. Mat. Astr. Fys.* **6**, no. 29.

Proudman, I. & Pearson, J. R. A. 1957 *J. Fluid Mech.* **2**, 237.

Roache, P. J. 1976 *Computational Fluid Dynamics*. Hermosa.

Schaaf, S. A. & Sherman, F. S. 1954 *J. Aero. Sci.* **21**, 85.

Schlamp, R. J., Pruppacher, H. R. & Hamielec, A. E. 1975 *J. Atmos. Sci.* **32**, 2330.

Takami, H. & Keller, H. B. 1969 *Phys. Fluids Suppl.* **12**, II-51.

Tamada, K. 1957 In *Proc. 9th Intl. Congr. Appl. Mech.* vol. 3, p. 343.